Food Chemistry: X 27 (2025) 102367

Contents lists available at ScienceDirect

Food Chemistry: X

journal homepage: www.sciencedirect.com/journal/food-chemistry-x

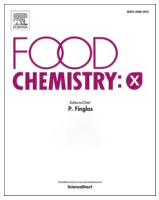

Untargeted metabolomics reveals flavor and metabolic changes in mixed Lactobacillus-fermented black mulberry juice

Mingshan Lv [1], Xiaolu Liu [1], Ruoqing Liu, Aihemaitijiang Aihaiti, Jingyang Hong, Li Zheng, Jun Xing, Yincang Cui, Liang Wang [*]

Collcge of Smart Agriculture (Rescarch Institute), Xinjiang University, Urumqi 830046, China

ARTICLE INFO

Keywords:
Black mulberries (*Morus nigra* L.)
Non-volatile flavor
Metabolomics
Fermentation
Mixed culture

ABSTRACT

This study aimed to investigate metabolic differences between mixed- and single-culture fermentation in black mulberry juice (BMJ). Using E-nose, E-tongue, and metabolomics, we analyzed metabolic profile variations and flavor compounds in BMJ fermented with different lactic acid bacteria (LAB). Results demonstrated that BMJ is an excellent fermentation substrate, with both cultures achieving colony counts exceeding 8 log CFU/mL after fermentation. Volcano plot and cluster analyses revealed that single-culture fermentation exhibited higher efficiency in biotransforming and degrading specific compounds, yet its metabolic profile was less diverse. In contrast, mixed-culture fermentation enhanced metabolic diversity through complementary pathways among strains, improving complex molecule production, optimizing flavors, reducing bitterness/astringency, and minimizing vitamin loss. This research provides a foundation for fermented mulberry beverage development. Future studies could integrate multi-omics analyses to advance industrial applications.

1. Introduction

Black mulberry (*Morus nigra* L.) has been widely distributed across tropical, subtropical, and temperate regions of the Northern Hemisphere since ancient times, providing significant economic value to local residents (Hosseini, Akramian, Khadivi, & Salehi-Arjmand, 2018). Introduced to China's Xinjiang region from Iran in the 16th century, the black mulberry quickly gained popularity due to its appealing taste and medicinal properties, leading to extensive cultivation. Today, over 100,000 mu (approximately 6666 ha) of mulberry trees are planted in Xinjiang. Black mulberries are rich in various natural antioxidants and prebiotics, receiving extensive investigation in modern biomedical and pharmacological research (Wen et al., 2019). Numerous studies have indicated that black mulberries offer significant health benefits, including enhancing muscle cell vitality, reducing organismal inflammation, and boosting cellular antioxidant activity (Donno, Cerutti, Prgomet, Mellano, & Beccaro, 2015). However, black mulberries also present a challenge. When they reach full ripeness, their pulp becomes soft and sweet. This characteristic unfortunately results in rapid spoilage after harvest. The swift spoilage poses substantial difficulties in handling and transportation processes, thereby restricting their commercial potential.

In recent years, lactic acid bacteria (LAB) have been widely used in functional food production to enhance the added value of food products (Shi et al., 2024). LAB fermentation not only imparts a distinct flavor to fruit juice but also biotransforms its bioactive compounds and enhances prebiotic properties (Guo et al., 2024). Previous studies have predominantly focused on the impact of single-strain fermentation on substrates. However, this single-strain fermentation approach has notable shortcomings. The substances produced by single-strain fermentation are relatively monotonous, and the utilization of substrates is insufficient. Moreover, slow metabolic rates and intermediate product accumulation prolong fermentation periods. Onsequently, research on mixed-strain fermentation has gained increasing attention in recent years. Recent studies have demonstrated significant advantages of mix-strain fermentation over single-strain fermentation. Specifically, multi-strain LAB co-fermentation systems exhibit superior growth dynamics and synergistic enhancement of metabolic products through interspecies interactions (Wang, Zhang, & Lei, 2022). In particular, mix-strain fermentation promotes the gradient synthesis of complex aromatic compounds, significantly enhancing the sensory profile of fermented beverages (Yu et al., 2024). Additionally, mixed-strain fermentation facilitates the conversion of large-molecule phenolic compounds in fruit

* Corresponding author.
E-mail address: WL1390593786@163.com (L. Wang).
[1] These authors contributed equally to this work.

https://doi.org/10.1016/j.fochx.2025.102367
Received 9 January 2025; Received in revised form 21 February 2025; Accepted 9 March 2025
Available online 17 March 2025

juices, such as procyanidins, into smaller bioactive components, including catechins, caffeic acid, and ferulic acid (Zhu et al., 2022). However, as the number of strains increases, the symbiosis and competition among microbial species in mixed fermentation become increasingly complex and uncertain. Previous research has mainly focused on co-fermentation with two to three strains of LAB, with limited metabolic studies on more diverse microbial communities. Nevertheless, such studies are crucial for the stable industrial production of LAB-based co-fermented products in the future.

Mixed-culture fermented black mulberry juice (FBMJ-Mix) is a plant-based beverage fermented by a mixture of *Lactobacillus paracasei* (LP), *Lactobacillus casei* (LC), *Lactobacillus plantarum* (LPL), *Lactobacillus fermentum* (LF), *Bifidobacterium animalis* subsp. *lactis* (BA), and *Lactobacillus delbrueckii* subsp. *bulgaricus* (LD). Early studies by our research group on FBMJ-Mix demonstrated that co-fermentation with these six strains of LAB significantly enhanced the enzymatic activity, phenolic compound content, and antioxidant properties of the juice (Lv et al., 2022). While these findings highlight the broad potential of co-fermented mulberry juice, systematic investigations into the metabolic mechanisms and pathways of multi-strain co-fermentation are lacking. This gap hinders further development of fermented mulberry juice as a functional fruit beverage. Therefore, understanding the characteristic changes in metabolites during these fermentation processes and clarifying the metabolic pathways of mixed fermentation will guide the industrial development of processed products.

Currently, diverse chromatographic techniques provide useful methods for the analysis of metabolites in fermented beverages (Zhong et al., 2022). Recent advancements in multi-omics technologies have significantly advanced research on food processing, preservation, and functional efficacy. These methodologies now provide a solid foundation for understanding the metabolic mechanisms of mixed-culture fermentation of black mulberry juice. In this study, advanced sensory and physicochemical analysis tools, such as electronic nose (E-nose), electronic tongue (E-tongue), and color difference meters, will be used to assess changes in the aroma and appearance of black mulberry juice (BMJ) during fermentation. Furthermore, an untargeted metabolomics approach utilizing UPLC-MS/MS technology will be implemented to investigate variations in the metabolic profiles of fermented black mulberry juice (FBMJ), influenced by different single strains and their combinations at various fermentation time intervals. The overarching objective is to elucidate the impact of single-strain and mixed-strain fermentation on the flavor and metabolic characteristics of the juice, as well as to delineate the functional roles and synergistic mechanisms of distinct bacterial strains within mixed fermentation systems.

2. Materials and methods

2.1. Materials

LAB including *Lactobacillus plantarum*, *Lactobacillus casei*, *Lactobacillus paracasei*, *Lactobacillus fermentum*, *Lactobacillus delbrueckii* subsp. *bulgaricus* and *Bifidobacterium animalis* subsp. *lactis* were obtained from Biobw Ltd. (Beijing, China). These black mulberries were sourced from a supermarket in Kuche City, Xinjiang, China. Pectinase, cellulase, and hemicellulase were sourced from Novozymes Biotech Ltd. (Tianjin, China). Methanol and acetonitrile were purchased from CNW Technologies (Ottawa, Canada), ammonium acetate from Sigma-Aldrich (St. Louis, USA), and acetic acid from Fisher Chemical (Pittsburgh, USA).

2.2. Bacterial culture

LAB were cultured in MRS liquid medium at 37 °C under anaerobic conditions for 24 h in a constant temperature incubator, and sub-cultured 2–3 times for subsequent use.

2.3. Preparation of FBMJ

The preparation method of FBMJ is detailed in a previously published study, including the selection of strain ratio and fermentation time (Lv et al., 2022). The process involves several steps: first, washing black mulberries to remove surface dust with distilled water. Next, use a blender to pulverize black mulberries into a uniform fruit puree. Then, adding 0.2 % (*w/v*) pectinase, 0.1 % (w/v) cellulase, and 0.1 % (w/v) hemicellulase, and conducting enzymatic hydrolysis at 55 °C for 3.5 h. The digested black mulberry juice (BMJ) was pasteurised at 85 °C for 30 min. After pasteurisation, the digested BMJ was inoculated at 37 °C. The total bacterial density in black mulberry juice was 6×10^6 CFU/mL. *Lactobacillus paracasei*, *Lactobacillus casei*, *Lactobacillus plantarum*, *Lactobacillus delbrueckii* subsp. *bulgaricus*, *Bifidobacterium animalis* subsp. *lactis*, and *Lactobacillus fermentum* were mixed in the ratio of 27.96 %, 15.37 %, 16.64 %, 5.12 %, 15.83 %, and 19.08 %. Finally, fermentation was conducted at 37 °C for 18 h.

2.4. Bacterial density counting

To determine the bacterial density in FBMJ, ensure that all apparatus and reagents are sterilized to mitigate the risk of contamination. The FBMJ sample should be diluted 100-fold for precise enumeration. Transfer a droplet of the diluted aliquot to the edge of a sterilized hemocytometer's counting chamber, allowing it to fill via capillary action without entrapping air bubbles. Position the hemocytometer beneath a microscope and, employing an appropriate magnification, count the bacteria within designated grids, typically comprising five grids (four corner quadrants and one central quadrant). Document the bacterial counts for each grid and compute the arithmetic mean:

$$Bacteria\ Density\ (cells/mL) = \frac{Counted\ Bacteria}{Number\ of\ Grids} \times Dilution\ Factor \times \frac{1}{Grid\ Volume} \quad (1)$$

where the grid volume is typically 0.1 mm^3 (10^{-4} mL). Document the calculated density for further analysis and quality control of the fermentation process.

2.5. Modeling the growth kinetics of LAB

Referring to the procedure for fitting the growth curve of lactic acid bacteria by Vasudha Sharma et al., to perform a nonlinear fitting of a lactic acid bacteria growth curve using GraphPad Prism v8.0.2 (GraphPad Software, San Diego, CA, USA) with the Gompertz growth model and obtain the fitted curve.

2.6. Physical and chemical indexes

2.6.1. E-tongue

The independent taste perception system (402B—C, Beijing Enovel Technology Development Co., Ltd., China) was employed to evaluate nine taste characteristics: sourness, bitterness, astringency, lingering astringency, lingering bitterness, umami, richness, saltiness, and sweetness. 40 mL of FBMJ from different fermentation stages was centrifuged at 2795*g* for 5 min at 25 °C. Subsequently, flavor measurements were conducted, with reference solutions serving as controls.

2.6.2. E-nose

The E-nose (C-PEN3, Beijing Enovel Technology Development Co., Ltd., China) was used to analyze the odor of fermented samples. This system comprises 10 metal oxide sensors, each designed to detect specific compounds such as aromatic benzene, nitrogen oxides, ammonia, hydrogen, aliphatic aromatic compounds, short-chain alkanes, sulfur compounds, terpenes, alcohols, aldehydes, ketones, organic sulfur

compounds, and long-chain alkanes. 10 mL of fermented samples were placed in 20 mL GC vials and incubated at room temperature for 30 min prior to measurement.

The detection parameters included a sample measurement time of 120 s, a cleaning time of 100 s, a pre-injection time of 5 s, a reset time of 5 s, and the carrier gas and injection flow rate were set at 200 mL/min. Data analysis was conducted using the E-nose software system.

2.6.3. Color difference

The color evaluation of fermented samples was conducted using a colorimeter (model DS-700D, Hangzhou Spectrum Technology Co., Ltd., Hangzhou, China), calibrated with a white reference plate.

2.6.4. Total reduced sugar content (RSC)

The RSC in the fermented sample was determined by the direct titration standard (Jiang et al., 2022). Methylene blue was used as an indicator, and the sample was titrated with a calibrated alkaline copper tartrate solution under heating to boiling conditions until the blue faded, and the RSC was calculated according to the consumption of sample solution using the following formula in Eq. (2) below:

$$X = \frac{m_1}{m \times F \times 10/250 \times 1000} \times 100 \quad (2)$$

where X is the RSC (g/100 g) of the sample, m_1 is the mass (mg) of the alkaline copper tartrate solution, m is the mass (g) of the sample, and F is a constant (1). The value of 10 referred to the volume (mL) of the sample solution, 250 referred to the constant volume (mL), and 1000 is the conversion factor.

2.6.5. Titratable Total acidity (TTA)

The method described by Amirdiavani and Baba (Amirdivani & Baba, 2011) was used to determine Titratable Total Acidity (TTA), with slight modifications. Initially, 2.5 g of FBMJ was mixed with 12.5 mL of distilled water in a homogenizer. Subsequently, 3 to 4 drops of 1 % phenolphthalein were added, and the mixture was titrated with 0.1 mol/L sodium hydroxide (NaOH) while being continuously stirred until a uniform pink color was achieved. The volume of sodium hydroxide used was recorded.

The TTA was calculated according to the consumption of sample solution using the following formula in Eq. (3) below:

$$Acidity(^{\circ}T) = V_{NaOH} \times 40 \quad (3)$$

2.7. LC-MS/MS method

The experimental method was adapted from Wu et al. (Wu et al., 2022), with optimizations. Initially, 300 μL of internal standard (methanol mixed with isotopically labeled internal standards) was added to 100 μL of sample for preparation. The mixture was sonicated (PS-60AL, Redbang Electronics Co., LTD, Shenzhen, China) and then incubated at −40 °C for 1 h. After centrifugation to remove protein precipitates, the supernatant was transferred to glass vials for analysis. UPLC-MS spectrometry (Vanquish, Thermo Fisher Scientific, Waltham, USA) was conducted using a UPLC HSS T3 column (2.1 mm × 100 mm, 1.8 μm). The mobile phase A in the chromatographic system consists of an aqueous solution containing 5 mmol/L ammonium acetate and 5 mmol/L acetic acid, while phase B is acetonitrile.

2.8. Statistical analysis

Untargeted metabolomics analysis was conducted on 11 independent samples ($n = 6$). Principal component analysis (PCA) and orthogonal partial least squares discriminant analysis (OPLS-DA) were performed using Metware Cloud, an online platform for data analysis (https://cloud.metware.cn). Hierarchical clustering analysis (HCA) was conducted using the R package ComplexHeatmap. Growth curve fitting and stacked bar graphs were generated using GraphPad Prism v8.0.2 (GraphPad Software, San Diego, CA, USA). Identified metabolites were annotated using the KEGG compound database and mapped to the KEGG pathway database. Other analyses were based on three independent experiments ($n = 6$), and data were processed using SPSS 22.0 (IBM, USA), followed by one-way analysis of variance (ANOVA) using Duncan's test. A p-value <0.05 was considered statistically significant.

3. Results and discussion

3.1. Growth curves of monoculture and mixed culture fermentation in black mulberry juice

The fermentation process of LAB is influenced by various factors, especially its adaptation to substrates, fermentation conditions, individual reproductive differences, etc., resulting in fermented products with different textures and flavors. Fitting bacterial growth curves can effectively monitor the fermentation process. Investigating whether BMJ meets the microbial growth and reproduction requirements is crucial (Zheng et al., 2023). Fig. 1 illustrates the fitted growth curves of different strains in BMJ. The curves demonstrate distinct growth patterns among different strains. Specifically, the LPL group reached the stationary phase most rapidly, while the LD group achieved the highest bacterial density during the stationary phase, indicating robust proliferation in this environment. For the Mix group, the prolonged lag phase suggests interactions among different microorganisms. However, by 18 h, Mix group entered the stationary phase with a bacterial density of 8.86×10^8, a two-order-of-magnitude increase from the initial inoculation density. This significant growth not only confirms BMJ as a suitable substrate for LAB fermentation but also demonstrates the feasibility of mixed culture fermentation in this environment, despite potentially longer initial adaptation periods.

3.2. Effect of LAB fermentation on the physicochemical properties of BMJ

3.2.1. E-tongue result analysis

E-tongue is a versatile detection method that plays a crucial role in understanding the taste attributes of beverages (Chen et al., 2023). Using the E-tongue, the descriptive features of the overall taste for each fermentation group were obtained. As shown in Fig. 2A, the FBMJ-Mix group exhibited different taste characteristics at different times. Compared to BMJ, the nine taste values of FBMJ at 18 h showed significant changes ($p < 0.05$). Fermentation time had a significant impact on the sweetness, sourness, bitterness, and astringency of FBMJ. The increase in acidity may be attributed to the large amount of organic acids produced by LAB through malolactic fermentation (Luo et al., 2024). As for single-strain fermentation (Fig. 2B), compared to FBMJ-Mix, single-strain fermentation resulted in significant changes in sweetness, sourness, astringency, bitterness, astringency, aftertaste A, and aftertaste B ($p < 0.05$). As shown in Fig. 2B, the trend of sweetness values for FBMJ-Mix decreased significantly from −13.64 to −15.98 (0 h vs 18 h), and the same trend was observed for other single-strain fermentations such as FBMJ-LC, FBMJ-LPL, FBMJ-LF, and FBMJ-BA, decreasing significantly from −13.64 to −15.94 (FBMJ-LF). Similarly, single-strain fermentation also contributed to a reduction in bitterness and astringency of FBMJ. Bitterness is closely related to the flavor of the juice. The reduction in bitterness of FBMJ-Mix might be due to the formation of a large amount of organic acids that masked the alternative flavors (Lao, Zhang, Li, & Bhandari, 2020). In terms of astringency, the sensor values for BMJ, FBMJ-Mix, and FBMJ-BA were 1.66, 1.43, and 1.09, respectively. The results indicate that mixed-culture fermentation altered the bitterness of the original juice, increased its acidity, and resulted in a more balanced flavor profile of FBMJ-Mix.

3.2.2. Electronic nose results analysis

E-nose analysis was conducted on FBMJ samples. As shown in the

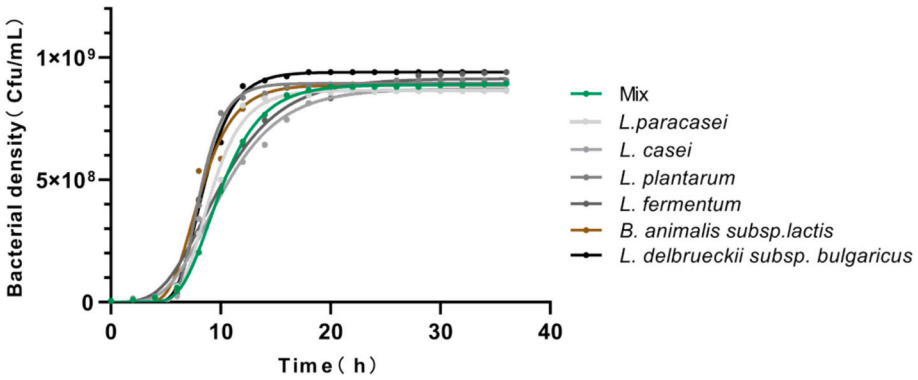

Fig. 1. Growth curves of monoculture and mixed culture fermentation in black mulberry juice.

radar chart (Fig. 2C), the sensors were sensitive to W1C, W5S, W1S, W2S, and W2W. This sensitivity represents an increase in the detection of aromatic components such as benzene compounds, nitrogen oxides, methyl compounds, alcohols, aldehydes, ketones, and organic sulfur compounds as fermentation time progressed. These substances are typical aromatic components found in black mulberry (Lv et al., 2023). Additionally, no sensitivity was observed for ammonia, hydrides, and alkanes in FBMJ. As fermentation time increased, more significant differences were observed in the sensor responses for FBMJ-Mix. Among them, BMJ showed the highest sensitivity to W2W, while at the end of fermentation, W1S exhibited the strongest sensitivity. Single-strain fermentation demonstrated similar sensor responses with FBMJ-Mix. However, FBMJ-LP, FBMJ-LD, and FBMJ-LPL (Fig. 2D) showed higher responses to various aromatic components, indicating that these three strains produced higher yields of volatile aromatic components. The results obtained from the electronic nose showed a high degree of similarity with those from GC–MS (X. Zhang, Tian, Xie, & Sun, 2022). Overall, significant differences were observed in the electronic nose responses for FBMJ at different fermentation times. This demonstrates that electronic nose technology can serve as a rapid and effective detection tool for monitoring odor changes during the fermentation process of FBMJ, thereby providing a reliable indicator to assess the degree of fermentation.

3.2.3. Color difference analysis

Color is a fundamental sensory indicator of juice. Fig. 2E-F show the changes in color difference parameters of FBMJ. Except for the FBMJ-LPL group, which showed an increase in L* values, all other groups experienced a decrease. The a* color parameter of FBMJ-Mix reached its lowest value between 18 h and 24 h. Compared to the initial fermentation, FBMJ-Mix had an insignificant effect on the L* value of BMJ. Among all the samples, FBMJ-LPL had the least impact on the a* value of BMJ, reducing it by 0.98, while the FBMJ-Mix group had the greatest impact, decreasing it by 2.64. The b* values of all fermented samples decreased, with the FBMJ-LP group showing the most significant reduction. The changes in the a* and b* values of the samples may be due to the decomposition and polymerization of colored compounds such as polyphenols and flavonoids. Overall, the trends in the changes of L*, a*, and b* color parameters during the fermentation of different strains were similar.

3.2.4. Analysis of Total acid and reducing sugar content

The changes in TTA and RSC values of FBMJ-Mix are shown in Fig. 2G. The TTA value of BMJ was initially 63.3°*T*, which increased to 68.6°*T* after mixed-strain fermentation. Compared to the FBMJ-Mix group, the single-strain fermentation groups exhibited lower sugar utilization rates. Combining this with the bacterial density data from Fig. 1, it can be seen that after 18 h, the reduction in sugar content and the increase in total acidity inhibited the specific growth rate of the bacteria. Additionally, the sugar utilization rate and acid production of the FBMJ-Mix group were significantly better than those of the single-strain fermentation groups.

3.3. Impact of LAB fermentation on the metabolomic profile of BMJ

Through metabolomics analysis, the impact of six strains of LAB fermentation on metabolites in BMJ was revealed. Principal component analysis (PCA) enabled the uncover hidden structures and patterns within the data, aiding in better understanding and interpretation (Y. Luo, Tang, Qiu, & Song, 2024). The principal component analysis plot with QC samples is shown in Fig. S1. The PCA score plot for all group metabolomics data (Fig. 3A) depicted three distinct clusters along the first and third principal components (PC-1 and PC-3), accounting for 24.48 % of the variance. This separation was based on the levels of metabolic activity during fermentation, with the positive end of PC-1 representing the control group, Mix-6 h, Mix-12 h, Mix-18 h, and Mix-24 h, and the negative end corresponding to the six monoculture fermented juices. Compared to the BMJ, Mix-6 h and Mix-12 h exhibited minimal metabolic activity. However, Mix-18 h and Mix-24 h, as well as the single-strain fermentation group, exhibited significant differences. LP, LC, LPL, LF, and BA were located on the positive end of PC-3, while LD was positioned on the negative end. The validation results of OPLS-DA are presented in Fig. S2, demonstrating good performance and reliable results. In the OPLS-DA results (Fig. 3B-C), Mix-18 h overlapped with LD and LP, while LF was the furthest component from Mix-18 h. This suggests the greatest compositional differences along the Component 1 axis between these groups.

The volcano plot visually displays metabolites that undergo significant changes under different conditions, aiding researchers in identifying and screening biologically meaningful differential metabolites (Zhao et al., 2024). Based on a *t*-test with a *p*-value <0.05 and an OPLS-DA model with a VIP score ≥ 1, differential metabolites were identified, resulting in the volcano plot shown in Fig. 4. As shown in Fig. 4, the early fermentation stages exhibited a marked predominance of upregulated metabolites over downregulated species, indicating heightened metabolic activity in mixed-culture BMJ fermentation. Notably, downregulated metabolites increased exponentially after 18 h.

Specifically, the levels of N-Acetyl-L-glutamate 5-phosphate, Feruloyldihydro-beta-sitosterol, and 15,15'-Dihydroxy-beta-carotene increased, while Atractyloside, 2,2′,5,5'-Tetrachlorobenzidine, dTDP-4-oxo-2,3,6-trideoxy-D-glucose, Lolicine A, TG(20:3/22:6/20:3), and Smilanippin A significantly decreased. These changes likely reflect the complex metabolic adaptation mechanisms of microorganisms during fermentation. For instance, the upregulation of 15,15'-Dihydroxy-beta-carotene may result from the cleavage of β-carotene by dioxygenases produced by the microbial community. This metabolite not only possesses direct antioxidant properties but can also be converted into vitamin A, enhancing the nutritional value of the fermented product

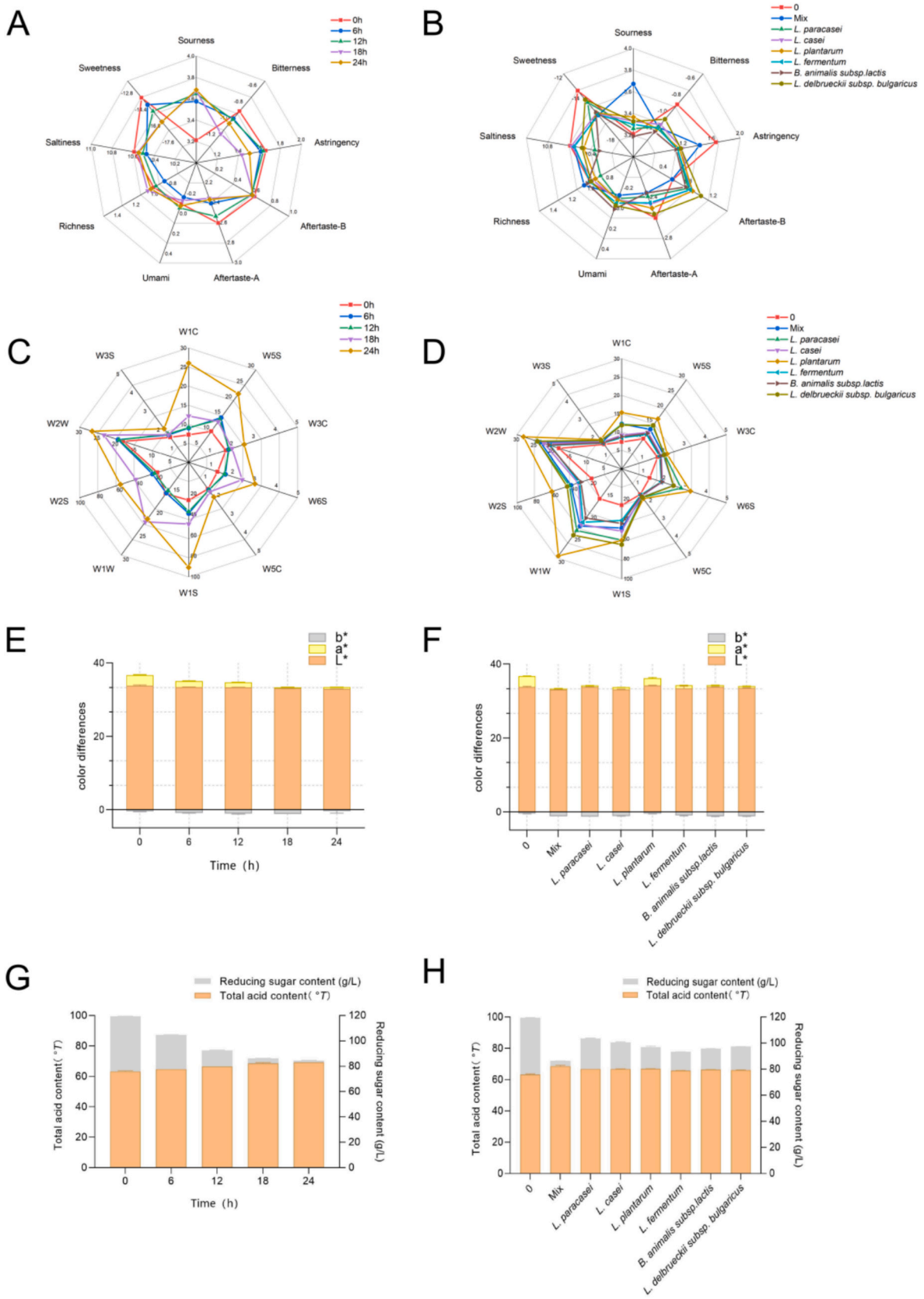

Fig. 2. Electronic tongue radar plots of FBMJ from mixed fermentation (A) and single-strain fermentation (B); electronic nose radar plots of FBMJ from mixed fermentation(C) and single-strain fermentation (D); color difference bar charts of FBMJ from mixed fermentation (E) and single-strain fermentation (F); bar charts of total acidity content and reducing sugar content in FBMJ from mixed fermentation (G) and single-strain fermentation (H).

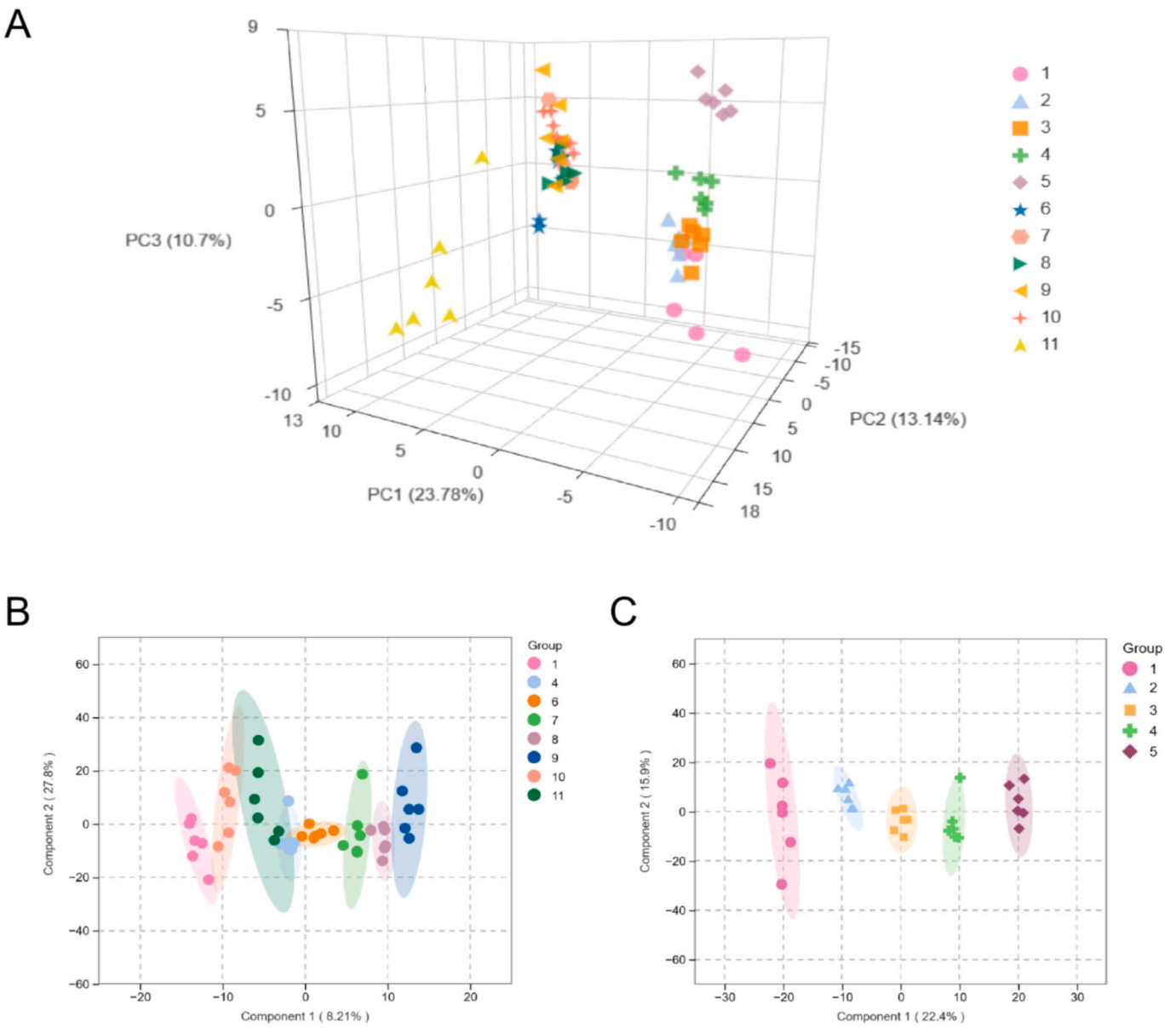

Fig. 3. A, PCA-3D plot of BMJ during mono-culture and co-culture fermentations at different time points; B, OPLS-DA plot of metabolites at the endpoint (18 h) of mono-culture and co-culture fermentation; C, OPLS-DA plot of metabolites at different time points of Mix group (1, BMJ; 2, Mix-6 h; 3, Mix-12 h; 4, Mix-18 h; 5, Mix-24 h; 6, LP; 7, LC; 8, LPL; 9, LF; 10, BA; 11, LD).

(Miao et al., 2024). Additionally, the downregulation of TG(20,3/22,6/20,3) may indicate microbial utilization of lipids as carbon or energy sources. Such metabolic remodeling likely influences final product characteristics including flavor profile, nutrient content, and shelf-life stability.

When comparing co-culture fermentation with monoculture conditions, over 5000 metabolites exhibited significant changes. After 18 h of mixed fermentation, 3'-AMP, Lolicine A, and 2,2′,5,5'-Tetrachlorobenzidine were significantly upregulated compared to single-strain fermentations, while Thiomorpholine 3-carboxylate, 7,8-Dihydromethanopterin, and Cyanidin 3,5,3′-tri-O-glucoside were generally downregulated. The upregulation of 3'-AMP likely reflects enhanced energy metabolism during mixed fermentation, consistent with findings from jujube juice (J. Li et al., 2024). Furthermore, the significant downregulation of sucrose in the mixed culture suggests its hydrolysis by fructosyltransferase, potentially serving as an energy source for lactic acid bacteria or for the biosynthesis of prebiotic fructo-oligosaccharides and polysaccharides (Xu, Hlaing, Glagovskaia, Augustin, & Terefe, 2020). The downregulation of Cyanidin 3,5,3′-tri-O-glucoside may be associated with glycoside hydrolysis and structural modifications of anthocyanins mediated by lactic acid bacteria. Overall, LAB fermentation drives the changing of the black mulberry metabolome through multiple coordinated pathways.

The proportions of each metabolite class are shown in Fig. 5A. Differential metabolites were selected based on VIP ≥ 1, $p < 0.05$ and FC ≥ 2 or FC ≤ 0.5 from all identified metabolites. The total of 911 differential metabolites were screened (Fig. 5A). These include lipids and lipid-like molecules (27.44 %, $n = 250$), phenylpropanoids and polyketides (13.28 %, $n = 121$), organoheterocyclic compounds (13.28 %, $n = 121$), organic acids and derivatives (20.20 %, $n = 184$), benzenoids (9.66 %, $n = 88$), organic oxygen compounds (8.01 %, $n = 73$), which together comprise over 90 % of the total differential metabolites. The remaining are composed of other (2.85 %, $n = 26$), organic nitrogen compounds (1.87 %, $n = 17$), nucleosides, nucleotides, and analogues (1.32 %, $n = 12$), alkaloids and derivatives (0.88 %, n = 8), lignans, neolignans and related compounds (0.55 %, $n = 5$), organosulfur compounds (0.22 %, n

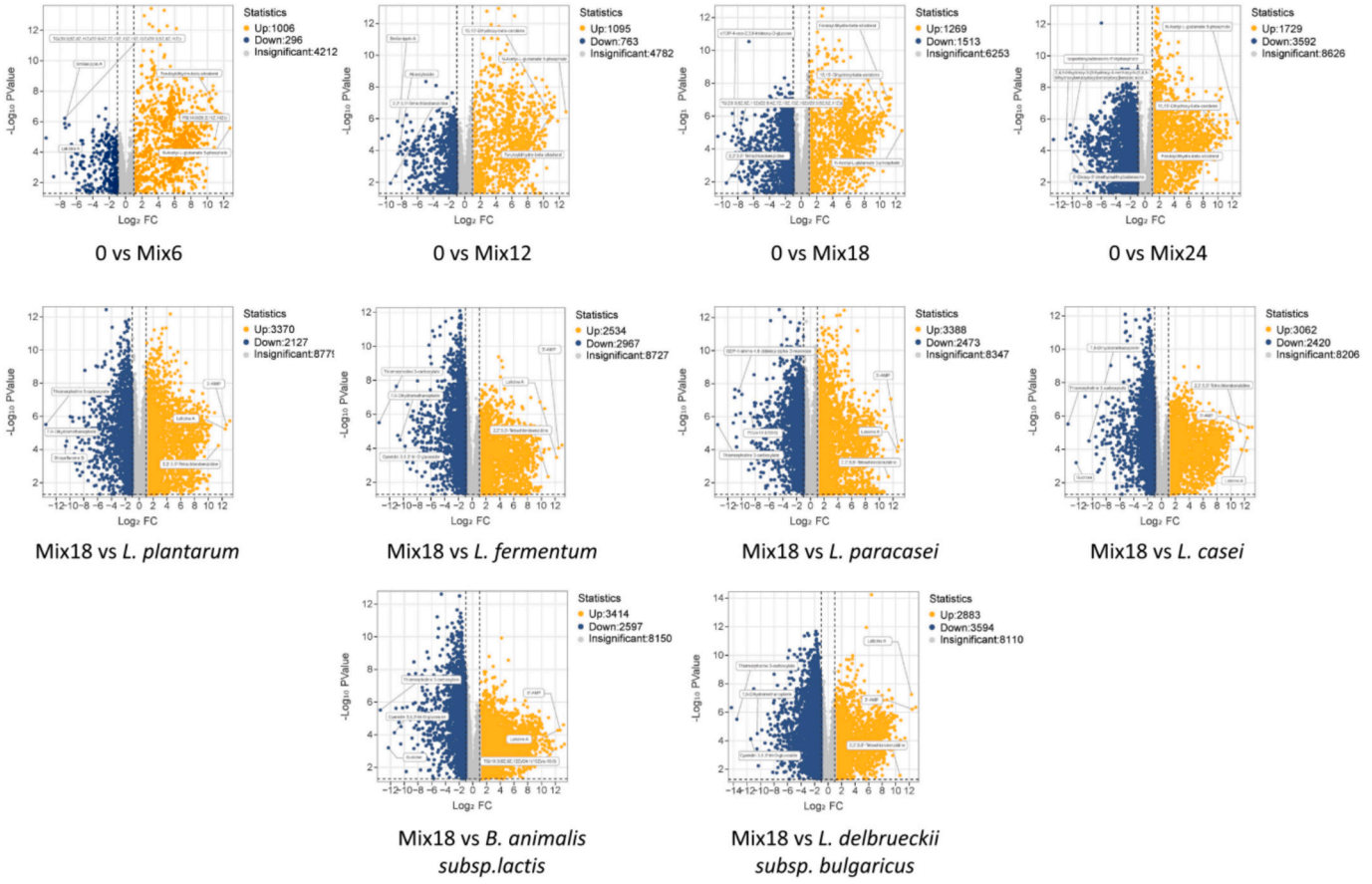

Fig. 4. Volcano plot of differential metabolites (yellow dots represent upregulated metabolites, blue dots represent downregulated metabolites, gray dots represent metabolites with no significant differences). (For interpretation of the references to color in this figure legend, the reader is referred to the web version of this article.)

= 2), hydrocarbons (0.33 %, n = 3), and homogeneous non-metal compounds (0.11 %, n = 1).

To analyze the changing trends of all differential metabolites, a K-means analysis was used to standardize and perform clustering analysis on the relative contents of the 911 differential metabolites. They were clustered into 9 different patterns of change, which were visualized in a clustering heatmap (Fig. 5B). Additionally, hierarchical clustering was performed on the metabolites from these 9 change patterns (Fig. 5C). The analysis revealed that among the single-strain fermentations, FBMJ-LPL group had the most significant fermentation effect, resulting in 268 up-regulated differential metabolites. There were 229 up-regulated differential metabolites in the Mix-18 h group. As shown in Fig. 5E, during the co-culture fermentation process, the proportion of lipid molecules and aromatic compounds increased, while the proportion of benzenoid, polyketide-like compounds, and organic acid-type compounds decreased.

3.3.1. *Lipids and lipid-like molecules and lignin*

Clustering analysis and heatmap plotting were performed for 80 types of lipids, lipid-like molecules, and lignin compounds. As shown in Fig. 6A, in the single-strain fermentation group, 25 lipid compounds, including Malabaricano, Sakacin P, LysoPE(18:3(6Z,9Z,12Z)/0:0), 16-Methylheptadecanoic acid, Cortisone, 5a-Pregnane-3,20-dione, Carissanol, 17-Hydroxypregnenolone sulfate, and Blennin D, were significantly downregulated. Moreover, as the fermentation time increased, a noticeable shift from orange to blue was observed in the heatmap. In the FBMJ-Mix group, the trend of lipid degradation was present but less pronounced, likely due to differences in resource allocation caused by competition or metabolic complementation between strains. Fatty acid compounds such as 16-Methylheptadecanoic acid and (9xi,10xi,12xi)-9,10-Dihydroxy-12-octadecenoic acid, as well as Methyl 2-heptenoate, were significantly accumulated in the mixed culture but showed no change in FBMJ-LF, FBMJ-BA, or FBMJ-LD.

Taurocholic acid was significantly increased in both single and mixed cultures, but showed higher accumulation in the mixed culture ($p < 0.01$). This may be related to the bile salt hydrolase activity of lactic acid bacteria (Tarique et al., 2022), which can convert conjugated bile acids into free forms. Lignan derivatives such as Carissanol and Secoisolariciresinol were uniquely accumulated in the mixed culture. This suggests that the mixed culture secretes complementary lignan peroxidases, which degrade mulberry lignans into diarylpropane compounds, which have higher added value. Furthermore, Secoisolariciresinol, as an antioxidant lignan, can enhance the stability and health benefits of the product when enriched (Masuda et al., 2010).

3.3.2. *Alkaloids, Phenylpropanoids, and polyketides, and Benzenoids*

Alkaloids, phenylpropanoids, polyketides, and aromatic compounds include phenols, phenyl ethers, aromatic compounds, and alkaloids, which are important antioxidants in black mulberry bioactive ingredients. Despite their beneficial properties, these substances can become toxic to cells at high doses. As shown in Fig. 6A, these compounds overall show a trend from orange to blue. Among 92 different substances analyzed, 22 compounds significantly decrease during mixed-fermentation. Most substances exhibit an overall decrease during fermentation, consistent with findings by Li et al., where phenolic compounds in kiwifruit significantly decreased after fermentation by LAB (Y. Li et al., 2024).

Compared to single-strain fermentation, in the FBMJ-Mix system, phenolic precursors such as phenylacetic acid and 3,4-dihydroxybenzylamine exhibited significant reductions, whereas bioactive molecules,

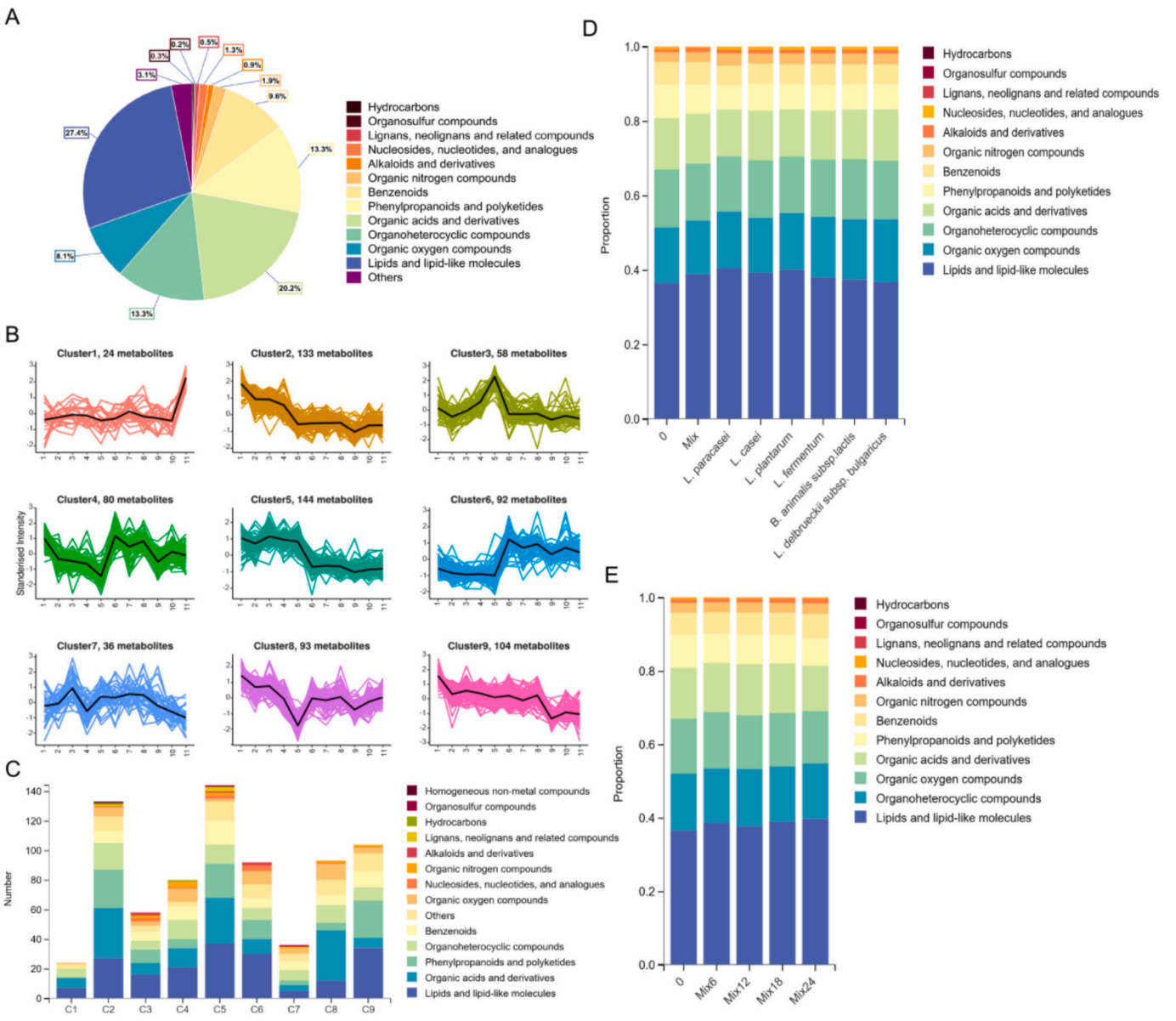

Fig. 5. A. Overall metabolite classification and their percentage composition; B. K-means clustering analysis of differential metabolites (1, BMJ; 2, Mix-6 h; 3, Mix-12 h; 4, Mix-18 h; 5, Mix-24 h; 6, LP; 7, LC; 8, LPL; 9, LF; 10, BA; 11, LD); C. Hierarchical clustering results of differential metabolites; D. Bar chart of differential metabolite classification in Mixed-FBMJ at different times fermentation. E. Bar chart of differential metabolite classification in FBMJ during monoculture fermentation by different strains.

including 3,4-dihydroxy-trans-cinnamate and orientin, showed notable increases. This observation suggests that the mixed-culture system employs a dual metabolic regulatory mechanism. During the degradation phase, LAB secreted phenolic acid decarboxylases (e.g., PAD), which metabolized complex phenolic compounds (e.g., maclurin) into anthocyanins, flavanols, and other phenolic compounds (Tang et al., 2023). In the synthesis phase, the mixed-culture system utilized cross-species glycosyltransferases to glycosylate decarboxylated products, leading to the formation of more stable compounds such as isoquercitrin. However, when fermentation was extended to 24 h, the concentrations of antioxidant molecules like quercitrin and orientin decreased, likely due to enzyme activity decay and oxidative losses.

Our comparative analysis revealed distinct metabolic pathways in flavonoid metabolism between mixed-culture fermentation and single-strain fermentation of FBMJ. Specifically, in FBMJ-LPL, macromolecular polyphenols such as emodin and rutin exhibited significant accumulation. The single LAB glycosidase system, which lacks diversity, is only capable of partial hydrolysis of the native bound flavonoids in mulberries. For instance, rutin is only partially converted to quercetin, with no further metabolism into smaller aglycone molecules (Leonard, Zhang, Ying, Adhikari, & Fang, 2021). In contrast, during mixed-culture fermentation, rutin was more likely to undergo bioconversion into kaempferol, ultimately yielding 4-hydroxybenzoic acid as the final product. Furthermore, the mixed-culture system demonstrated enhanced catalytic activity in producing methylated derivatives like Isorhamnetin, which exhibit increased bioavailability (Yang et al., 2023).

In summary, despite the reduction in most phenolic compounds, this decrease did not negatively impact the bioactivity of FBMJ (Lv et al., 2025). Conversely, the bioactive potential of the FBMJ-Mix group was enhanced, primarily attributed to the microbial-mediated conversion of flavonoids into glycosylated derivatives with elevated antioxidant activity. Furthermore, compared to single-strain fermentation, mixed-culture fermentation demonstrated greater efficiency in liberating

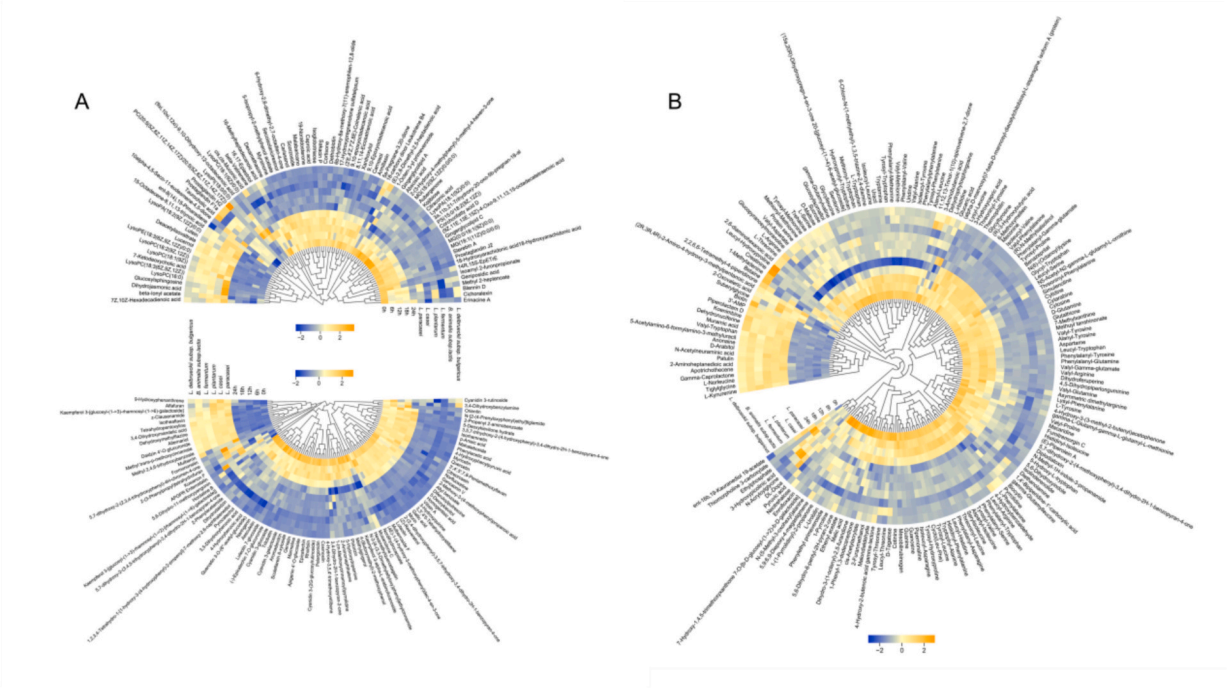

Fig. 6. A. Clustering heatmap of lipids and lipid-like molecules, lignin (top), phenylpropanoids and polyketides, alkaloids and aromatic compounds (bottom); B. Heatmap of other organic compounds.

bound caffeic acid and quinic acid from chlorogenic acid. It also achieved a more extensive metabolic conversion of flavonoid derivatives into aglycones and subsequent methylation, processes that collectively contribute to the enhanced antioxidant activity of FBMJ.

3.3.3. *Organic acids and derivatives*

Metabolomics revealed distinct strategies in organic acid and amino acid metabolism between single-culture and mixed-culture systems (Fig. 6B). In single-culture fermentation (e.g., FBMJ-BA), malic acid content significantly decreased, primarily due to its efficient conversion into lactic acid via specific transformation mechanisms (Table S1). In contrast, the mixed-culture system likely utilized malic acid in the tricarboxylic acid cycle to produce succinic acid, thereby reducing the efficiency of lactic acid conversion. Single-culture fermentation mitigates the sharp acidity of the juice by accumulating lactic acid, whereas the mixed-culture system retains malic acid, contributing to a smoother fruit aroma (Ji et al., 2023).

Regarding amino acid metabolism, single-culture systems uniquely degraded leucine to produce α-ketoisocaproic acid, while mixed-culture systems biotransformed tryptophan into indole-3-lactic acid, which possesses bitterness-reducing propertie. The dynamic fluctuation of aspartic acid in mixed-culture systems suggests competitive utilization of its precursors among microbial strains. Sweet compounds, such as phenylalanyl-serine and glycine, significantly decreased in single-culture groups, possibly due to the involvement of free glycine in browning reactions or its role as a carbon source supporting microbial

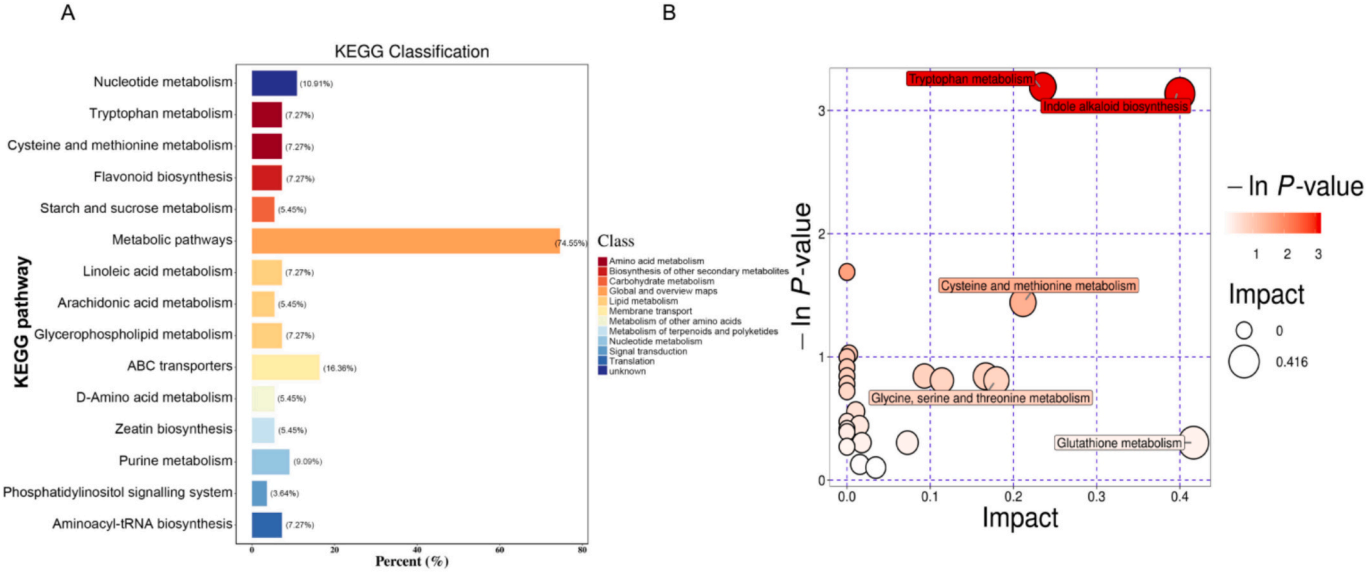

Fig. 7. A. KEGG Pathway Enrichment Analysis of Differential Metabolites in FBMJ;B. Influence Factor Diagram of KEGG Enrichment Analysis.

growth. Phenylalanine levels decreased in mixed-culture groups and positively correlated with flavonoid synthesis, as it serves as a precursor in the biosynthesis of flavonoid compounds (Leonard et al., 2021). In terms of peptide metabolism, single-culture groups showed a significant increase in isoleucyl-valine, while mixed-culture systems reorganized flavor-related peptides through intermolecular interactions among microbial communities, leading to elevated levels of umami compounds, such as glutamate.

3.3.4. *Organic oxygen compounds*

The metabolic dynamics of carbohydrate compounds during BMJ lactic acid fermentation exhibited distinct microbial community-specific characteristics (Fig. 6B). In unfermented BMJ, primary carbohydrates such as β-D-glucosamine generally decreased after fermentation, while D-arabitol significantly accumulated across all fermentation groups, suggesting that mixed-culture lactic acid fermentation may serve as a potential microbial system for D-arabitol production (Ravikumar et al., 2022).

Notably, maltotriose degradation efficiency in FBMJ-Mix only marginally surpassed by some single-culture groups, indicating that multi-microbial synergy did not significantly enhance the utilization efficiency of this polysaccharide. However, rare sugar metabolism showed divergent patterns. L-erythrulose exhibited the most significant degradation in the mixed-culture group, whereas it increased in the LPL single-culture group.

Regarding flavor precursor compounds, phenylethyl primeveroside decreased in all fermentation groups, with its degradation potentially linked to the release of aroma compounds (Ouyang et al., 2022).

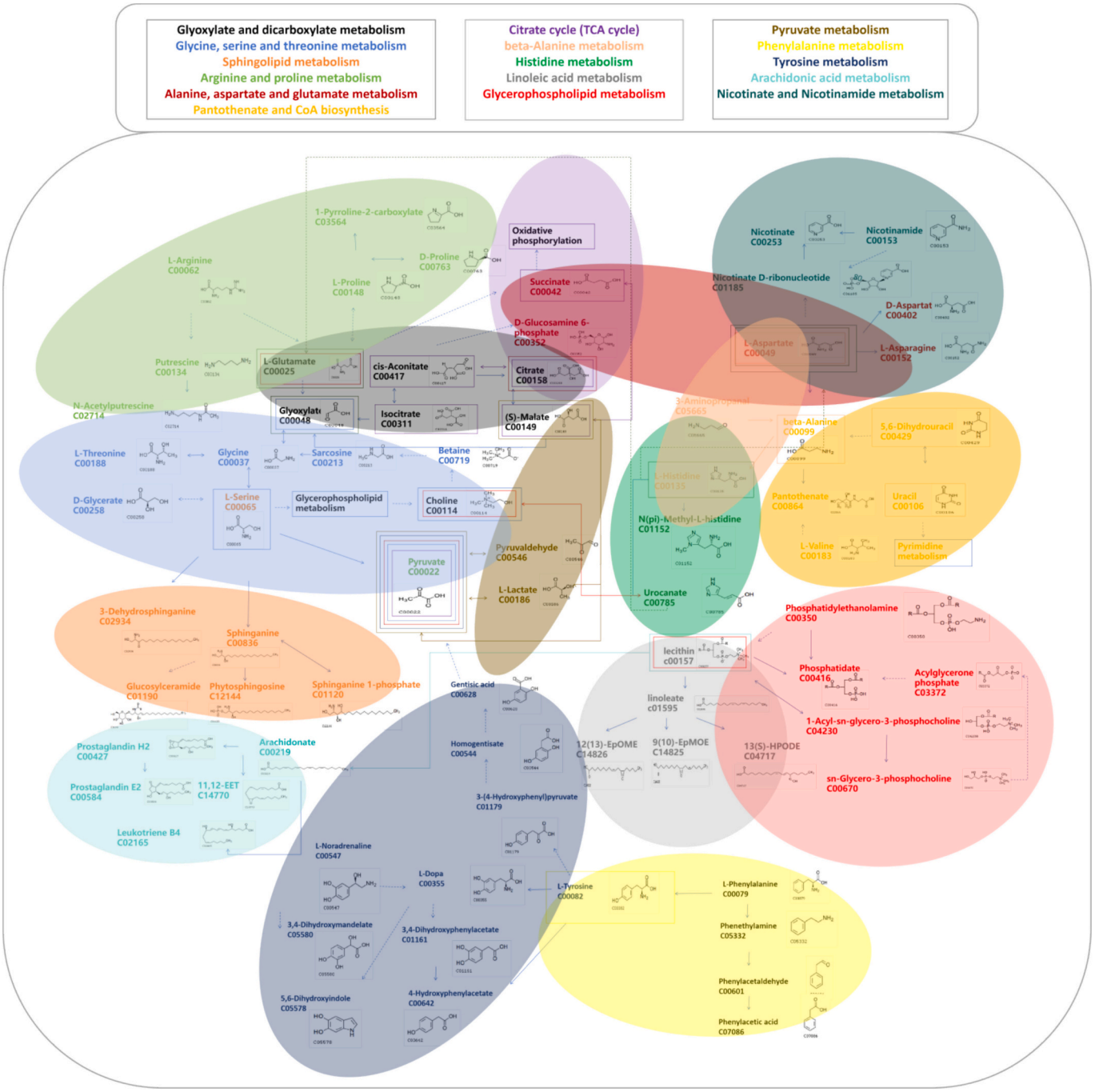

Fig. 8. Metabolic pathway network of differential metabolites in FBMJ.

Furthermore, glucosylisomaltol degradation was most pronounced in the mixed-culture group, with a lower retention rate compared to the LD single-culture group. This highlights the cooperative hydrolytic advantage of mixed-culture systems for glycosidic compounds (Liang et al., 2024). Notably, the LF group specifically accumulated D-arabitol and L-erythrulose, indicating a unique metabolism in the strain of rare sugars.

3.3.5. *Organic heterocyclic compounds*

Heterocyclic compounds are widely distributed in nature, with many important biological compounds falling into this category, such as nucleic acids, certain vitamins, antibiotics, hormones, pigments, and alkaloids. A total of 121 heterocyclic compounds were found among the differential metabolites in FBMJ. Among these, 82 compounds exhibit overlapping metabolic trends between mixed-culture and single-strain groups, with 47 heterocyclic compounds downregulated across all groups (Table. S1).

In terms of vitamin metabolism, biotin levels significantly increased in both single-culture and mixed-culture groups, likely due to enhanced biosynthetic capabilities of the microbial strains. However, thiamine only accumulated in the single-culture group. Pyridoxine, niacinamide, and pantothenic acid levels generally decreased, likely due to the dynamic consumption of cofactors during metabolic processes. Notably, the FBMJ-Mix group uniquely upregulated 19 heterocyclic compounds, including cytidine and 6,7-Dimethyl-8-(1-D-ribityl)lumazine. In contrast, the single-culture group predominantly accumulated purine degradation products, such as hypoxanthine. The richness of lactic acid bacteria shows a positive correlation with purine metabolism, and previous studies have also demonstrated the therapeutic potential of these bacteria in managing metabolic disorders (Song, Zhou, Li, Huang, & Zhou, 2024).

3.4. *KEGG annotation and enrichment analysis of differential metabolites*

Pathway enrichment analysis for the metabolites of FBMJ was performed using the KEGG database, targeting mulberry (*Morus*) as the species of interest. The analysis revealed that the largest number of annotations were associated with general metabolism pathways (Fig. 7).

Using the KEGG database, a total of 57 metabolic pathways were

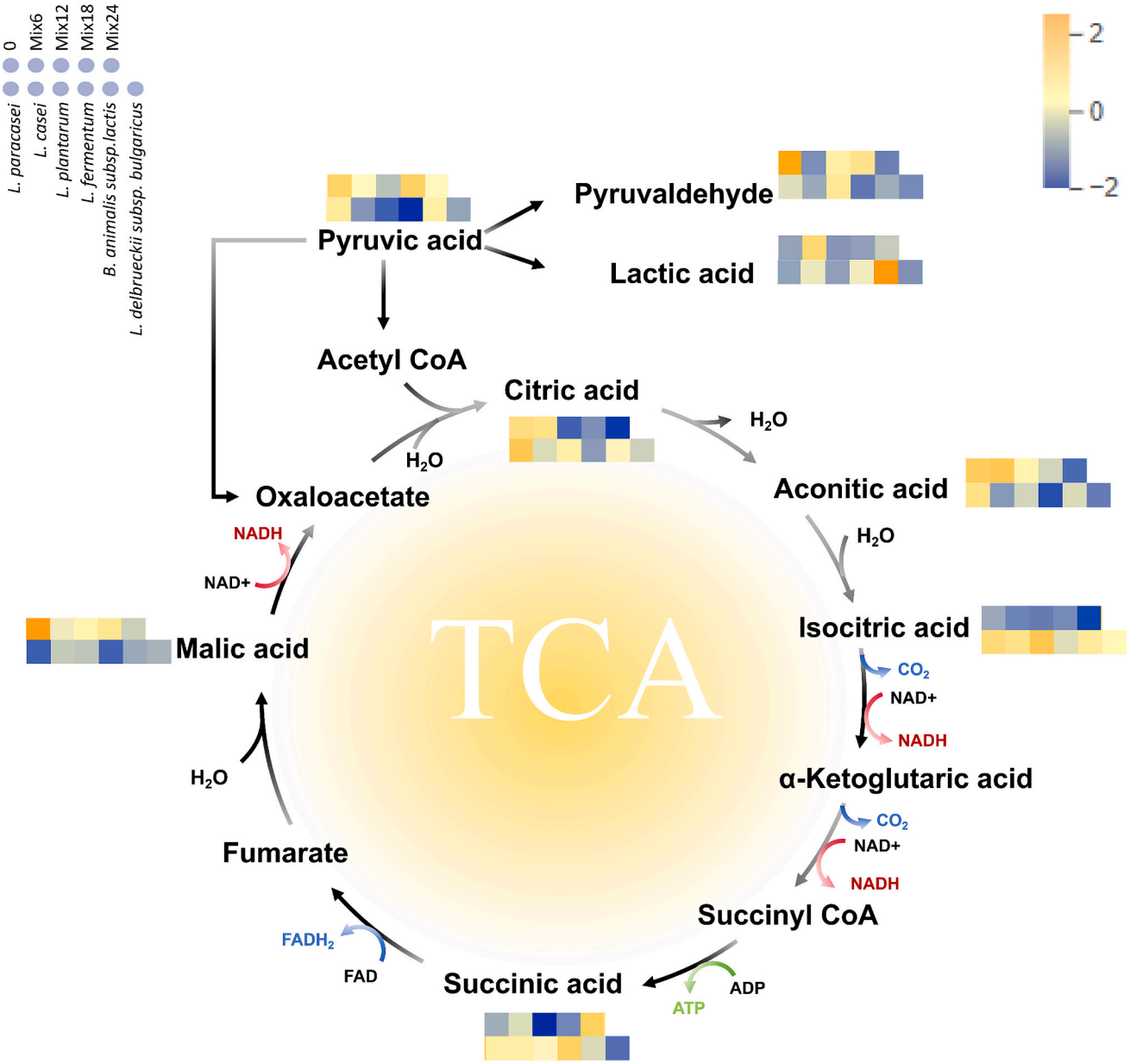

Fig. 9. Tricarboxylic acid cycle and pyruvate metabolism network of differential metabolites in FBMJ.

identified through enrichment analysis of differential metabolites in FBMJ. Further enrichment analysis of differential metabolite pathways identified 16 pathways with p-values <0.05 (Fig. 8).

Acetaldehyde and dicarboxylate metabolism is one of the important metabolic processes in organisms. Acetaldehyde in FBMJ, a simple two-carbon acid, serves as an intermediate in many metabolic pathways, significantly downregulated to acetyl-CoA during fermentation (Fig. 8), and subsequently participates in the TCA cycle. The TCA cycle is the central hub of substance metabolism in organisms (Y. J. Zhang & Fernie, 2018). This pathway begins with glucose or other fermentable sugars being broken down into pyruvate through glycolysis (Fig. 9). Under aerobic conditions, pyruvate undergoes further oxidation to produce energy, while under anaerobic fermentation conditions, pyruvate is converted to lactate catalyzed by lactate dehydrogenase. This reaction not only regenerates NAD^+, an essential cofactor for sustaining glycolysis, but also produces lactate as the final product. Analysis of pyruvate conversion and metabolites annotated in the TCA cycle (Fig. 9) revealed decreased levels of pyruvate and acetaldehyde in the Mix-6 group, accompanied by the accumulation of lactate. Additionally, succinic acid and malic acid levels increased, while citric acid and malic acid levels gradually decreased. By the end of fermentation (Mix-18), significant accumulation of succinic acid was observed. In single-strain fermentation, significant accumulation of lactate was notably observed in BA group, and sensory analysis indicated that malic acid provides a sharper taste, which transforms into lactate to enhance product flavor (Taniasuri, Lee, & Liu, 2016). Pyruvate occupies a central position in the metabolic network and participates in the majority of metabolic pathways (Fig. 8). In the late fermentation stage of black mulberry juice, after complex metabolic processes by LAB, pyruvate begins to accumulate and shows an upregulation, while glycine, serine, and threonine are converted as nitrogen sources into pyruvate and glyceric acid or enter sphingolipid metabolism to produce metabolites such as 3-dehydrosphinganine and sphinganine. Glycine, serine, and threonine metabolism not only provide necessary nutrition and energy during lactic acid fermentation but also support the growth, fermentation, and product formation of LAB by regulating metabolic pathways and biosynthetic processes. It is noteworthy that some metabolites in the alanine, aspartate and glutamate metabolism pathway, such as L-aspartic acid, D-glucosamine 6-phosphate, and succinate, are simultaneously present in the tricarboxylic acid cycle and nicotinate and nicotinamide metabolism pathways. Meanwhile, L-aspartic acid also serves as a core metabolic product in β-alanine metabolism and histidine metabolism pathways to maintain metabolic balance and growth rate of LAB (Kajitani et al., 2022). Another pathway worth noting is the phenylalanine metabolism pathway and tyrosine metabolism pathway, where flavonoid compounds are initiated by phenylalanine in the biosynthesis process to produce phenylalanine, which then enters the flavonoid-anthocyanin pathway (N. Jiang, Doseff, & Grotewold, 2016). Following mixed-culture fermentation, chalcone isomerase in the flavonoid-cyanidin pathway catalyzes the production of naringenin, which is subsequently carboxylated to form dihydroquercetin, eventually yielding quercetin (Table S1), thereby generating diverse anthocyanins from various flavonols. On the other hand, starting from phenylalanine entering the tyrosine metabolic pathway (Fig. 8), significant accumulation of L-dopa occurs in the LD group, while significant accumulation of L-norepinephrine occurs in the BA group. Throughout the entire fermentation process, levels of L-phenylalanine and phenylethylamine decrease significantly, while levels of benzaldehyde and 3,4-dihydroxyphenylacetic acid ester increase notably. Paying attention to these substances may elucidate potential bioactive factors during the fermentation of black mulberry juice.

4. Conclusion

This study utilized LC-MS/MS to analyze the metabolic impact of single and mixed LAB fermentation on mulberry juice. The results demonstrated that multi-strain interactions significantly influenced functional diversity and sensory properties through metabolic cooperation or competition. Mixed-culture fermentation enhanced metabolite diversity via complementary pathways among strains, showcasing a superior ability to produce complex molecules, such as the enrichment of lignan lactones. Compared to single-culture fermentation, mixed fermentation optimized flavor profiles by enhancing acid production and metabolizing bitter peptides from BMJ. However, single-culture fermentation exhibited higher efficiency in biotransforming specific compounds; for instance, *Lactobacillus plantarum* degraded most of the bitter amino acids in BMJ while accumulating thiamine. Mixed fermentation also reduced certain lipid oxidation losses and synthesized new biologically active small-molecule phenols. Analysis of fermentation stages indicated that the 12–18 h period maximized the production of flavonoid glycosides and bioactive peptides, whereas post-24 h fermentation led to increased oxidative losses. These findings support the use of mixed-culture systems for functional beverages and single-culture fermentation for nutrient fortification. Future studies should integrate metagenomics to advance precision fermentation.

CRediT authorship contribution statement

Mingshan Lv: Writing – original draft, Software, Methodology, Conceptualization. **Xiaolu Liu:** Software, Data curation. **Ruoqing Liu:** Investigation, Data curation. **Aihemaitijiang Aihaiti:** Writing – review & editing. **Jingyang Hong:** Writing – review & editing. **Li Zheng:** Writing – review & editing. **Jun Xing:** Writing – review & editing. **Yincang Cui:** Writing – review & editing. **Liang Wang:** Writing – review & editing, Conceptualization.

Declaration of competing interest

The authors declare that they have no known competing financial interests or personal relationships that could have appeared to influence the work reported in this paper.

Acknowledgments

This research was funded by Research on Key Technologies for Refined Deep Processing of Xinjiang characteristic subsidiary agricultural products, Autonomous Region Key Research and Development Program Sub-project (2022B02026-3), Excellent doctoral Scientific Research and Innovation Program of Xinjiang University (XJU2022BS052) and Xinjiang Autonomous Region Graduate Innovation Project (XJ2023G030).

Appendix A. Supplementary data

Supplementary data to this article can be found online at https://doi.org/10.1016/j.fochx.2025.102367.

Data availability

Data will be made available on request.

References

Amirdivani, S., & Baba, A. S. (2011). Changes in yogurt fermentation characteristics, and antioxidant potential and in vitro inhibition of angiotensin-1 converting enzyme upon the inclusion of peppermint, dill and basil. *LWT - Food Science and Technology, 44*(6), 1458–1464.

Chen, L., Ning, F., Zhao, L., Ming, H., Zhang, J., Yu, W., Yi, S., & Luo, L. (2023). Quality assessment of royal jelly based on physicochemical properties and flavor profiles using HS-SPME-GC/MS combined with electronic nose and electronic tongue analyses. *Food Chemistry, 403*, Article 134392.

Donno, D., Cerutti, A. K., Prgomet, I., Mellano, M. G., & Beccaro, G. L. (2015). Foodomics for mulberry fruit (*Morus spp.*): Analytical fingerprint as antioxidants' and health properties' determination tool. *Food Research International, 69*, 179–188.

Guo, S., Sun, Y., Wu, T., Kwok, L.-Y., Sun, Z., Wang, J., & Zhang, H. (2024). Co-fermented milk beverage has better stability and contains more health-promoting amino acid metabolites than single-strain-fermented milk beverage over one-month storage. *Food Chemistry, 430*, Article 136840.

Hosseini, A.-S., Akramian, M., Khadivi, A., & Salehi-Arjmand, H. (2018). Phenotypic and chemical variation of black mulberry (*Morus nigra*) genotypes. *Industrial Crops and Products, 117*, 260–271.

Ji, G., Liu, G., Li, B., Tan, H., Zheng, R., Sun, X., & He, F. (2023). Influence on the aroma substances and functional ingredients of apple juice by lactic acid bacteria fermentation. *Food Bioscience, 51*, Article 102337.

Jiang, N., Doseff, A. I., & Grotewold, E. (2016). Flavones: From biosynthesis to health benefits. *PLANTS-BASEL, 5*(2).

Jiang, X., Tian, J., Huang, H., Hu, X., Han, L., Huang, D., & Luo, H. (2022). Nondestructive visualization and quantification of total acid and reducing sugar contents in fermented grains by combining spectral and color data through hyperspectral imaging. *Food Chemistry, 386*, Article 132779.

Kajitani, K., Ishikawa, T., Kobayashi, T., Asato, M., Shibata, K., Kouya, T., & Takahashi, S. (2022). Mechanism of high D-aspartate production in the lactic acid bacterium *Latilactobacillus* sp. strain WDN19. *Applied Microbiology and Biotechnology, 106*(7), 2651–2663.

Lao, Y., Zhang, M., Li, Z., & Bhandari, B. (2020). A novel combination of enzymatic hydrolysis and fermentation: Effects on the flavor and nutritional quality of fermented Cordyceps militaris beverage. *LWT, 120*, Article 108934.

Leonard, W., Zhang, P., Ying, D., Adhikari, B., & Fang, Z. (2021). Fermentation transforms the phenolic profiles and bioactivities of plant-based foods. *Biotechnology Advances, 49*, Article 107763.

Li, J., Xu, H., Li, H., Xie, Y., Ding, K., Xu, S., … Ding, S. (2024). Co-fermentation of *Lactiplantibacillus* and *Streptococcusccus* enriches the key-contribution volatile and non-volatile components of jujube juice. *Food Research International, 196*, Article 115093.

Li, Y., Wang, W., Deng, Y., Gao, J., Shi, J., & Cai, L. (2024). Antioxidant properties and changes *in vitro* digestion of the fermented kiwifruit extract prepared by lactic acid bacteria and yeasts. *Food Chemistry, 442*, Article 138416.

Liang, W., Wang, X., Zhang, L., Jiao, S., Song, H., Sun, J., & Wang, D. (2024). Changes and biotransformation mechanism of main functional compounds during kombucha fermentation by the pure cultured tea fungus. *Food Chemistry, 458*, Article 140242.

Luo, J.-W., Xiao, S., Suo, H., Wang, B., Cai, Y.-X., & Wang, J.-H. (2024). Dynamics of nutrients, sensory quality and microbial communities and their interactions during co-fermentation of pineapple by-products and whey protein. *Food Chemistry: X, 22*, Article 101254.

Luo, Y., Tang, R., Qiu, H., & Song, A. (2024). Widely targeted metabolomics-based analysis of the impact of *L. plantarum* and *L. paracasei* fermentation on rosa roxburghii Tratt juice. *International Journal of Food Microbiology, 417*, Article 110686.

Lv, M., Aihaiti, A., Liu, X., Tuerhong, N., Yang, J., Chen, K., & Wang, L. (2022). Development of probiotic-fermented black mulberry (*Morus nigra* L.) juice and its antioxidant activity in C2C12 cells. *Fermentation, 8*(12), 697.

Lv, M., Liu, X., Chen, K., Aihaiti, A., Maimaitiyiming, R., Xing, J., … Wang, L. (2023). Effects of adding milk to fermented black mulberry (*Morus nigra* L.) juice on its antioxidant activity in C2C12 cells and changes in volatile flavor compounds during storage. *Food Chemistry X, 20*, Article 101029.

Lv, M., Liu, X., Liu, R., Aihaiti, A., Hong, J., Zheng, L., Xing, J., Cui, Y., & Wang, L. (2025). Analysis of the antioxidant efficacy substances in fermented black mulberry juice and their preventive effects on oxidative stress in C2C12 cells. *Food Chemistry, 473*, Article 142988.

Masuda, T., Akiyama, J., Fujimoto, A., Yamauchi, S., Maekawa, T., & Sone, Y. (2010). Antioxidation reaction mechanism studies of phenolic lignans, identification of antioxidation products of secoisolariciresinol from lipid oxidation. *Food Chemistry, 123*(2), 442–450.

Miao, Q., Si, X., Zhao, Q., Zhang, H., Qin, Y., Tang, C., & Zhang, J. (2024). Deposition and enrichment of carotenoids in livestock products: An overview. *Food Chemistry: X, 21*, Article 101245.

Ouyang, W., Yu, Y., Wang, H., Jiang, Y., Hua, J., Ning, J., & Yuan, H. (2022). Analysis of volatile metabolite variations in strip green tea during processing and effect of rubbing degree using untargeted and targeted metabolomics. *Food Research International, 162*, Article 112099.

Ravikumar, Y., Razack, S. A., Ponpandian, L. N., Zhang, G., Yun, J., Huang, J., … Qi, X. (2022). Microbial hosts for production of D-arabitol: Current state-of-art and future prospects. *Trends in Food Science & Technology, 120*, 100–110.

Shi, H., Zhao, Y., Wang, W., Zhou, Y., Liang, Y., Wu, R., & Wu, J. (2024). The potential of lactic acid bacteria in fermented herbs-derived food products. *Food Bioscience, 61*, Article 104714.

Song, X., Zhou, Q., Li, X., Huang, Q., & Zhou, Y. (2024). Spontaneous fermentation tunes purine metabolism of tomato by modifying bacterical diversity: Based on metabonomics and microbiomics. *LWT, 191*, Article 115486.

Tang, S., Luo, N., Zeng, Q., Dong, L., Zhang, R., He, S., … Su, D. (2023). Lychee pulp phenolics fermented by mixed lactic acid bacteria strains promote the metabolism of human gut microbiota fermentation *in vitro*. *Food & Function, 14*(16), 7672–7681.

Taniasuri, F., Lee, P.-R., & Liu, S.-Q. (2016). Induction of simultaneous and sequential malolactic fermentation in durian wine. *International Journal of Food Microbiology, 230*, 1–9.

Tarique, M., Abdalla, A., Masad, R., Al-Sbiei, A., Kizhakkayil, J., Osaili, T., Olaimat, A., Liu, S.-Q., Fernandez-Cabezudo, M., & al-Ramadi, B., & Ayyash, M.. (2022). Potential probiotics and postbiotic characteristics including immunomodulatory effects of lactic acid bacteria isolated from traditional yogurt-like products. *LWT, 159*, Article 113207.

Wang, L., Zhang, H., & Lei, H. (2022). Phenolics profile, antioxidant activity and flavor volatiles of pear juice: Influence of lactic acid fermentation using three *Lactobacillus* strains in monoculture and binary mixture. *Foods, 11*.

Wen, P., Hu, T.-G., Linhardt, R. J., Liao, S.-T., Wu, H., & Zou, Y.-X. (2019). Mulberry: A review of bioactive compounds and advanced processing technology. *Trends in Food Science & Technology, 83*, 138–158.

Wu, T. Y., Liang, J., Ai, J. Y., Cui, J. L., Huang, W. D., You, Y. L., & Zhan, J. C. (2022). Mulberry ethanol extract and Rutin protect alcohol-damaged GES-1 cells by inhibiting the MAPK pathway. *Molecules, 27*(13).

Xu, Y., Hlaing, M. M., Glagovskaia, O., Augustin, M. A., & Terefe, N. S. (2020). Fermentation by probiotic *Lactobacillus gasseri* strains enhances the carotenoid and fibre contents of carrot juice. *Foods, 9*.

Yang, F., Chen, C., Ni, D., Yang, Y., Tian, J., Li, Y., … Wang, L. (2023). Effects of fermentation on bioactivity and the composition of polyphenols contained in polyphenol-rich foods: A review. *Foods, 12*.

Yu, Q., Qian, J., Xu, Q., Guo, Y., Yao, W., Qian, H., & Cheng, Y. (2024). Integration of cross-correlation analysis and untargeted flavoromics reveals unique flavor formation of lactic acid bacteria co-fermented oat beverage. *Food Bioscience, 59*, Article 103855.

Zhang, X., Tian, W., Xie, B., & Sun, Z. (2022). Insight into the influence of lactic acid Bacteria fermentation on the variations in flavor of chickpea Milk. *Foods, 11*.

Zhang, Y. J., & Fernie, A. R. (2018). On the role of the tricarboxylic acid cycle in plant productivity. *Journal of Integrative Plant Biology, 60*(12), 1199–1216.

Zhao, X., Wang, Z., Tang, F., Cai, W., Peng, B., & Shan, C. (2024). Exploring jujube wine flavor and fermentation mechanisms by HS-SPME-GC–MS and UHPLC-MS metabolomics. *Food Chemistry: X, 21*, Article 101115.

Zheng, Z., Wei, L., Zhu, M., Qian, Z., Liu, J., Zhang, L., & Xu, Y. (2023). Effect of lactic acid bacteria co-fermentation on antioxidant activity and metabolomic profiles of a juice made from wolfberry and longan. *Food Research International, 174*, Article 113547.

Zhong, P., Wei, X. Q., Li, X. M., Wei, X. Y., Wu, S. Z., Huang, W. J., … Lei, H. T. (2022). Untargeted metabolomics by liquid chromatography-mass spectrometry for food authentication: A review. *Comprehensive Reviews in Food Science and Food Safety, 21*(3), 2455–2488.

Zhu, Y., Lv, J., Gu, Y., He, Y., Chen, J., Ye, X., & Zhou, Z. (2022). Mixed fermentation of Chinese bayberry pomace using yeast, lactic acid bacteria and acetic acid bacteria: Effects on color, phenolics and antioxidant ingredients. *LWT, 163*, Article 113503.